Direct Sequence Spread Spectrum Walsh-QPSK Modulation

Dongwook Lee, *Member, IEEE,* Hun Lee, and Laurence B. Milstein, *Fellow, IEEE*

***Abstract*— In this paper we present Walsh-quadrature phase-shift keying (Walsh-QPSK) pseudonoise (PN) modulation schemes for both coherent and noncoherent direct-sequence code-division multiple-access (DS-CDMA) systems, wherein the PN spreading sequences for in-phase and quadrature data in a conventional QPSK PN modulation scheme are coded by Walsh sequences indexed by a special rule to reduce the envelope variation of the transmitted signal. Signal characteristics of the two schemes are analyzed when a rectangular-shaped PN chip pulse is used, and it is shown that the proposed coherent DS-CDMA system has a constant envelope even in the presence of a transmitted phase reference. We simulate the signals to obtain the envelope variations when a spectrally efficient shaped PN chip pulse is used, and compare the results with those of conventional QPSK and orthogonal QPSK (OQPSK) PN modulation schemes. The results show that both the noncoherent and coherent Walsh-QPSK schemes have smaller envelope variations than the conventional noncoherent QPSK and OQPSK PN modulation schemes, even though in the coherent Walsh-QPSK scheme the pilot channel is added to the signal channel.**

***Index Terms*—CDMA, direct-sequence, spread-spectrum communications, Walsh-QPSK modulation.**

I. Introduction

SEVERAL versions of direct-sequence code-division multiple-access (DS-CDMA) have been proposed for cellular, personal communications services (PCS) and wireless local loop (WLL) applications [1]–[5]. Important requirements for a portable terminal in wireless applications with mobility are low cost, low power consumption, small size, and light weight. To meet the requirements of low power consumption, an efficient power amplifier should be used. From the point of view of service providers, spectral efficiency is also an important requirement. However, usually a spectrally efficient signal has a large envelope variation. The large envelope variation of the transmitted signal results in increased adjacent channel interference and degraded system performance due to spectral regeneration at the output of a nonlinear power amplifier [6].

Both noncoherent M-ary orthogonal signaling for data modulation with orthogonal quadrature phase-shift keying (OQPSK) pseudonoise (PN) spreading [5] and coherent QPSK data modulation with QPSK PN spreading [2] have been proposed for a DS-CDMA portable terminal. Using noncoherent OQPSK PN modulation, there is some self-interference between the in-phase and quadrature components resulting from a delay of a half PN chip duration in the quadrature component of the transmitted signal, although it is typically much smaller than the multiple access interference from the other users [7]. Using coherent QPSK PN modulation, the system might require a pilot channel for coherent demodulation. Further, the sum of the pilot channel and the signal channel exhibits a high envelope variation and a large phase change.

In this paper a special case of QPSK PN modulation, called Walsh-QPSK, is investigated to see if it can exhibit lower envelope variation and smaller phase changes than the conventional PN modulation schemes proposed in [1]–[5].

The Walsh-QPSK PN modulation uses a property of the product of two adjacent indexed Walsh sequences, which is derived in Section II. Section III presents system models of the Walsh-QPSK PN modulations for both noncoherent and coherent systems. In Section IV signal characteristics of these systems are analyzed when a rectangular-shaped PN chip pulse is used. In Section V we perform simulations to determine the envelope variations of the proposed system models and compare them with those of conventional schemes when the spectrally efficient shaped PN chip pulse proposed in [5] is used. Finally, we present the conclusions in Section VI.

II. Property of the Product of Two Adjacent Indexed Walsh Sequences

In this section we derive a property of the product of two adjacent indexed Walsh sequences. It is well known that the Hadamard matrices can be generated by means of the following recursive procedure [8]:

$$\mathbf{H_1} = [0] \qquad \mathbf{H}_2 = \begin{bmatrix} 0 & 0 \\ 0 & 1 \end{bmatrix} \qquad \mathbf{H}_{2M} = \begin{bmatrix} \mathbf{H}_M & \mathbf{H}_M \\ \mathbf{H}_M & \overline{\mathbf{H}}_M \end{bmatrix} \quad (1)$$

where $M = 2^P$ for any nonnegative integer P and $\overline{\mathbf{H}}_M$ denotes the binary complement of $\mathbf{H}_M$. The (m, n)th element of the matrix $\mathbf{H}_M$ is denoted by $wal(m, n)$. The Walsh sequence with index of m is denoted by $W_n^m(n = \cdots, -2, -1, 0, 1, 2, \cdots)$,

Paper approved by C. Robertson, the Editor for Spread Spectrum Systems of the IEEE Communications Society. Manuscript received March 4, 1997; revised January 30, 1998. This work was supported by the Electronics and Telecommunications Research Institute (ETRI), Taejon, Korea.

D. Lee is with the Department of Electrical and Computer Engineering, University of California at San Diego, La Jolla, CA 92093-0407 USA, on leave from the Electronics and Telecommunications Research Institute (ETRI), Taejon 305-350 Korea (e-mail: dwlee@ece.ucsd.edu).

H. Lee is with the Mobile Communications Division, Electronics and Telecommunications Research Institute (ETRI), Taejon 305–350, Korea (e-mail: hlee@etri.re.kr).

L. B. Milstein is with the Department of Electrical and Computer Engineering, University of California at San Diego, La Jolla, CA 92093–0407 USA (e-mail: milstein@ece.ucsd.edu).

Publisher Item Identifier S 0090-6778(98)06646-X.

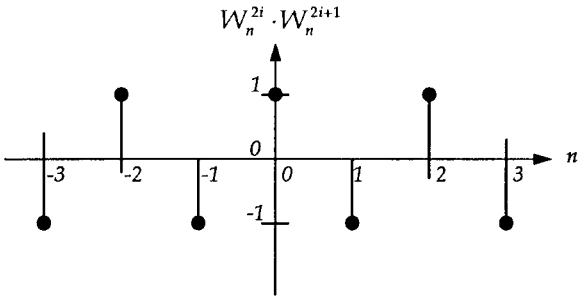

Fig. 1. Product of two adjacent indexed Walsh sequences.

where $W_n^m = wal(m, n \bmod(M))$ for $n \geq 0$ and $W_n^m = wal(m, M - |n| \bmod(M))$ for $n < 0$.

The $wal(m, n)$ and the W_n^m take on the real values ± 1, rather than the values zero and one over $GF(2)$, with the following standard mapping relating the two:

$$\begin{array}{ccc} GF(2) & & \text{Reals} \\ 0 & \Longleftrightarrow & +1 \\ 1 & \Longleftrightarrow & -1. \end{array} \tag{2}$$

The factored expression of $wal(m, n)$ derived in [8] is given by

$$wal(m, n) = (-1)^{j_{P-1}k_{P-1}} \cdot (-1)^{j_{P-2}k_{P-2}} \cdots (-1)^{j_0 k_0} \tag{3}$$

where $(j_{P-1}, j_{P-2}, \cdots, j_0)$ and $(k_{P-1}, k_{P-2}, \cdots, k_0)$ are binary representations for m and n, respectively, and are given by $m = \sum_{p=0}^{P-1} 2^p j_p$ and $n = \sum_{p=0}^{P-1} 2^p k_p$. Note that j_p and k_p have the value of zero or one. We obtain the product of W_n^{2i} and $W_n^{2i+1} (i = 0, 1, 2, \cdots, M/2 - 1)$ from (3) as

$$W_n^{2i} \cdot W_n^{2i+1} = (-1)^{k_0} = (-1)^n. \tag{4}$$

Note that in (4) the product of W_n^{2i} and W_n^{2i+1} is not a function of i, but only a function of n. The product of the $(2i)$th and $(2i+1)$th Walsh sequences is shown in Fig. 1.

III. System Model

A. Noncoherent DS-Spread-Spectrum Walsh-QPSK System

In general, assuming that there are N chips per data symbol, a QPSK PN signal is given by [9]

$$S_{\text{QPSK}}(t) = \sqrt{S} \sum_{n=-\infty}^{\infty} h(t - nT_c)\{d^c_{\lfloor n/N \rfloor} c^c_n \cos(\omega_c t) + d^s_{\lfloor n/N \rfloor} c^s_n \sin(\omega_c t)\} \tag{5}$$

where $d^c_{\lfloor n/N \rfloor}$ and $d^s_{\lfloor n/N \rfloor}$ are the in-phase and quadrature data sequences, respectively, c^c_n and c^s_n are corresponding binary PN sequences, S is the transmit power, $1/T_c$ is the chip rate, and $h(t)$ is the impulse response of the chip-shaping filter.

Fig. 2 shows the block diagram of a noncoherent DS-spread-spectrum Walsh-QPSK system (NWQPSK) transmitter. It can be seen that NWQPSK is a special case of QPSK PN modulation, where $d^c_{\lfloor n/N \rfloor} = d^s_{\lfloor n/N \rfloor} = d_{\lfloor n/N \rfloor}$, $c^c_n = c_n W_n^{2i}$, $c^s_n = c_n W_n^{2i+1}$, and c_n is a binary PN sequence. Therefore, the transmitted signal $S_{\text{NWQPSK}}(t)$ is given by

$$S_{\text{NWQPSK}}(t) = \sqrt{S} \sum_{n=-\infty}^{\infty} h(t - nT_c)\{d_{\lfloor n/N \rfloor} c_n W_n^{2i} \cdot \cos(\omega_c t) + d_{\lfloor n/N \rfloor} c_n W_n^{2i+1} \sin(\omega_c t)\}. \tag{6}$$

B. Coherent DS-Spread-Spectrum Walsh-QPSK System

Fig. 3 shows the block diagram of a coherent DS-spread-spectrum Walsh-QPSK (CWQPSK) transmitter. To separate the pilot and signal channels, different pairs of Walsh sequences are used in each channel. Further, one of the four Walsh sequences is multiplied by -1 to reduce the envelope variation of the transmitted signal. The transmitted signal $S_{\text{CWQPSK}}(t)$ is given by

$$S_{\text{CWQPSK}}(t) = \sum_{n=-\infty}^{\infty} h(t - nT_c) \cdot c_n \left\{ \begin{array}{l} \left(\sqrt{S_D}\, d_{\lfloor n/N \rfloor} W_n^{2i} + \sqrt{S_P} W_n^{2j}\right) \cos(\omega_c t) \\ \quad + \left(\sqrt{S_D}\, d_{\lfloor n/N \rfloor} W_n^{2i+1} - \sqrt{S_P} W_n^{2j+1}\right) \\ \quad \cdot \sin(\omega_c t) \end{array} \right\} \tag{7}$$

where S_D and S_P are the data and pilot signal transmit powers, respectively, and $i \neq j$. Note that from (4), $W_n^{2i} = (-1)^n W_n^{2i+1}$. Therefore, (7) can be rewritten as

$$S_{\text{CWQPSK}}(t) = \sum_{n=-\infty}^{\infty} h(t - nT_c) \cdot c_n \left\{ \begin{array}{l} \left(\sqrt{S_D}\, d_{\lfloor n/N \rfloor} W_n^{2i} + \sqrt{S_P}\, W_n^{2j}\right) \cos(\omega_c t) \\ \quad + (-1)^n \left(\sqrt{S_D}\, d_{\lfloor n/N \rfloor} W_n^{2i} - \sqrt{S_P}\, W_n^{2j}\right) \\ \quad \cdot \sin(\omega_c t) \end{array} \right\}. \tag{8}$$

In this equation we observe that if the sum of the in-phase signals is constructive, then the sum of the quadrature signals is destructive, and vice versa. This property can reduce the envelope variation of $S_{\text{CWQPSK}}(t)$, as will be seen below. Indeed, note that by using a rectangular-shaped PN chip pulse, i.e., $h(t) = 1$ for $0 \leq t < T_c$ and $h(t) = 0$ otherwise, the envelope of the signal has a constant value of $\sqrt{2(S_D + S_P)}$.

IV. Signal Characteristics

A. NWQPSK

To test the constellation of NWQPSK, we consider the in-phase and quadrature sequences in (6). From (6), the in-phase sequence I_n^{NWQPSK} and the quadrature sequence Q_n^{NWQPSK} are given by

$$I_n^{\text{NWQPSK}} = d_{\lfloor n/N \rfloor} c_n W_n^{2i} \tag{9a}$$

and

$$Q_n^{\text{NWQPSK}} = d_{\lfloor n/N \rfloor} c_n W_n^{2i+1} \tag{9b}$$

respectively. From (4), (9b) can be rewritten as

$$Q_n^{\text{NWQPSK}} = (-1)^n d_{\lfloor n/N \rfloor} c_n W_n^{2i} = (-1)^n I_n^{\text{NWQPSK}}. \tag{10}$$

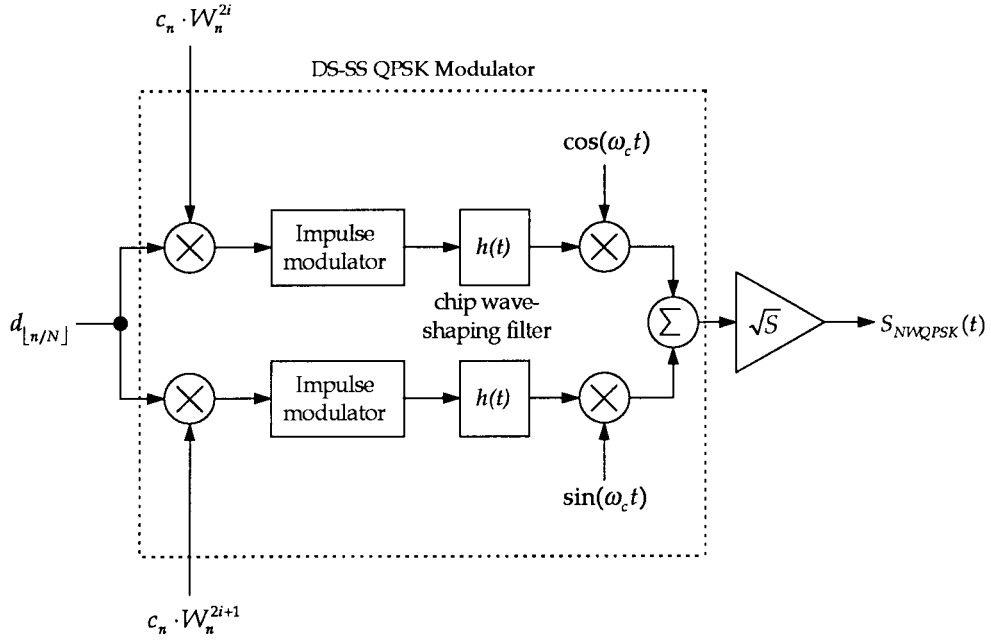

Fig. 2. Block diagram of NWQPSK.

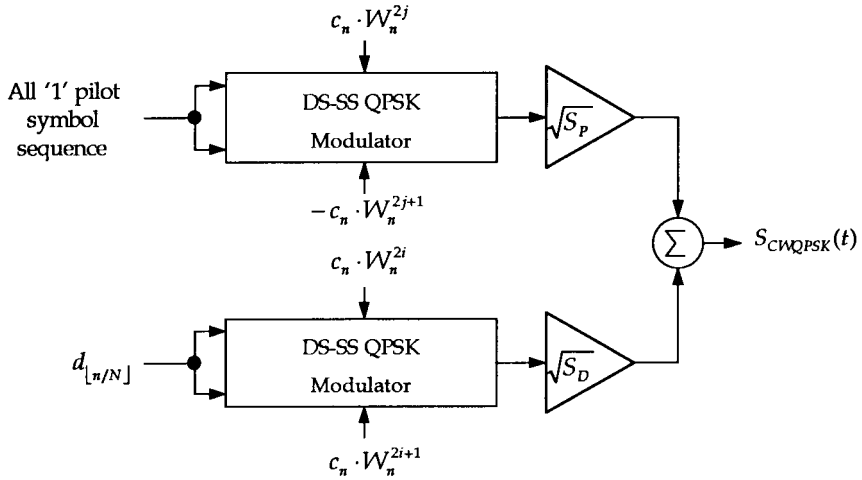

Fig. 3. Block diagram of CWQPSK.

If n is an even number, then possible pairs of $(I_n^{\mathrm{NWQPSK}}, Q_n^{\mathrm{NWQPSK}})$ are (1, 1) and $(-1, -1)$. If n is an odd number, then the possible pairs are $(1, -1)$ and $(-1, 1)$. Therefore, the signal constellation of NWQPSK becomes as shown in Fig. 4. The phase difference at the sample point is always $\pi/2$ or $-\pi/2$, which is similar to the signal constellation of OQPSK. Furthermore, with NWQPSK under ideal conditions, there is no self-interference between the in-phase and quadrature sequences, since the in-phase and quadrature sequences are orthogonal because of the orthogonality of the Walsh sequences.

B. CWQPSK

From (8), the in-phase sequence I_n^{CWQPSK} and the quadrature sequence Q_n^{CWQPSK} are given by

$$I_n^{\mathrm{CWQPSK}} = c_n\left(\sqrt{S_D}\, d_{\lfloor n/N \rfloor} W_n^{2i} + \sqrt{S_P}\, W_n^{2j}\right) \quad (11a)$$

and

$$Q_n^{\mathrm{CWQPSK}} = (-1)^n c_n\left(\sqrt{S_D}\, d_{\lfloor n/N \rfloor} W_n^{2i} - \sqrt{S_P}\, W_n^{2j}\right) \quad (11b)$$

respectively. These two sequences are no longer $+1$ or -1. Equation (11) can be rewritten as

$$I_n^{\mathrm{CWQPSK}} = \sqrt{S_D}\, c_n^1 + \sqrt{S_P}\, c_n^2 \quad (12a)$$

and

$$Q_n^{\mathrm{CWQPSK}} = (-1)^n\left(\sqrt{S_D}\, c_n^1 - \sqrt{S_P}\, c_n^2\right) \quad (12b)$$

where $c_n^1 = c_n d_{\lfloor n/N \rfloor} W_n^{2i}$ and $c_n^2 = c_n W_n^{2j}$. We define two sets S_1 and S_2 where S_1 and S_2 represent the possible pairs of $(I_n^{\mathrm{CWQPSK}}, Q_n^{\mathrm{CWQPSK}})$ when n is odd and when n is even, respectively. From (12), the elements of S_1 and S_2 are given

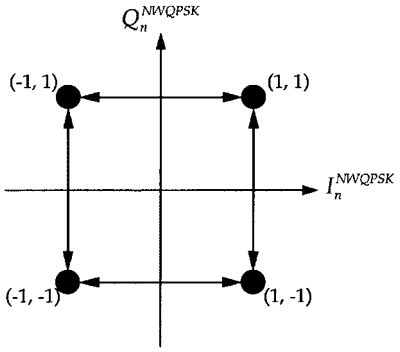

Fig. 4. Signal constellation of NWQPSK.

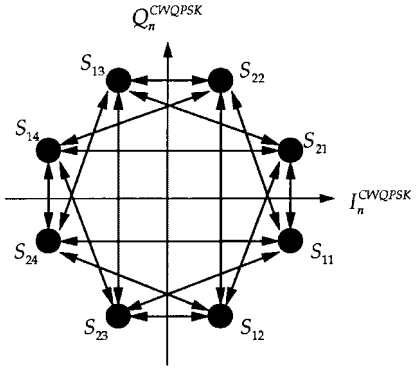

Fig. 5. Signal constellations of CWQPSK assuming $S_D > S_P$.

by

$$\begin{aligned}
S_{11} &\equiv (I_n^{\mathrm{CWQPSK}}, Q_n^{\mathrm{CWQPSK}})|_{n=\mathrm{odd},\, c_n^1=1,\, c_n^2=1} \\
&= \left(\sqrt{S_D}+\sqrt{S_P}, -\sqrt{S_D}+\sqrt{S_P}\right), \\
S_{12} &\equiv (I_n^{\mathrm{CWQPSK}}, Q_n^{\mathrm{CWQPSK}})|_{n=\mathrm{odd},\, c_n^1=1,\, c_n^2=-1} \\
&= \left(\sqrt{S_D}-\sqrt{S_P}, -\sqrt{S_D}-\sqrt{S_P}\right), \\
S_{13} &\equiv (I_n^{\mathrm{CWQPSK}}, Q_n^{\mathrm{CWQPSK}})|_{n=\mathrm{odd},\, c_n^1=-1,\, c_n^2=1} \\
&= \left(-\sqrt{S_D}+\sqrt{S_P}, \sqrt{S_D}+\sqrt{S_P}\right), \\
S_{14} &\equiv (I_n^{\mathrm{CWQPSK}}, Q_n^{\mathrm{CWQPSK}})|_{n=\mathrm{odd},\, c_n^1=-1,\, c_n^2=-1} \\
&= \left(-\sqrt{S_D}-\sqrt{S_P}, \sqrt{S_D}-\sqrt{S_P}\right) \qquad (13)
\end{aligned}$$

and

$$\begin{aligned}
S_{21} &\equiv (I_n^{\mathrm{CWQPSK}}, Q_n^{\mathrm{CWQPSK}})|_{n=\mathrm{even},\, c_n^1=1,\, c_n^2=1} \\
&= \left(\sqrt{S_D}+\sqrt{S_P}, \sqrt{S_D}-\sqrt{S_P}\right), \\
S_{22} &\equiv (I_n^{\mathrm{CWQPSK}}, Q_n^{\mathrm{CWQPSK}})|_{n=\mathrm{even},\, c_n^1=1,\, c_n^2=-1} \\
&= \left(\sqrt{S_D}-\sqrt{S_P}, \sqrt{S_D}+\sqrt{S_P}\right), \\
S_{23} &\equiv (I_n^{\mathrm{CWQPSK}}, Q_n^{\mathrm{CWQPSK}})|_{n=\mathrm{even},\, c_n^1=-1,\, c_n^2=1} \\
&= \left(-\sqrt{S_D}+\sqrt{S_P}, -\sqrt{S_D}-\sqrt{S_P}\right), \\
S_{24} &\equiv (I_n^{\mathrm{CWQPSK}}, Q_n^{\mathrm{CWQPSK}})|_{n=\mathrm{even},\, c_n^1=-1,\, c_n^2=-1} \\
&= \left(-\sqrt{S_D}-\sqrt{S_P}, -\sqrt{S_D}+\sqrt{S_P}\right) \qquad (14)
\end{aligned}$$

respectively. We consider four cases: case 1) $c_n^1 = c_n^2$ and $c_{n+1}^1 = c_{n+1}^2$; case 2) $c_n^1 = -c_n^2$ and $c_{n+1}^1 = -c_{n+1}^2$; case 3) $c_n^1 = -c_n^2$ and $c_{n+1}^1 = c_{n+1}^2$; and case 4) $c_n^1 = c_n^2$ and $c_{n+1}^1 = -c_{n+1}^2$. The constellation points for case 1 are S_{11}, S_{14}, S_{21}, and S_{24}. Since n increases in time by one unit, the constellation point moves from either S_{11} or S_{14} for n an odd number, to either S_{21} or S_{24} for n an even number, or vice versa. Therefore, for case 1, the constellation point moves on the rectangle S_{11}–S_{21}–S_{14}–S_{24}. In a similar manner, for case 2, the constellation point moves on the rectangle S_{12}–S_{22}–S_{13}–S_{23}. For cases 3 and 4, the constellation point moves on the rectangles S_{12}–S_{21}–S_{13}–S_{24} and S_{11}–S_{22}–S_{14}–S_{23}, respectively. Assuming $S_D > S_P$, the signal constellation of CWQPSK is shown in Fig. 5. Note that in cases 3 and 4 the constellation point moves around a square, as in NWQPSK. Also note that when $S_D = S_P$, we have $S_{11} = S_{21}$, $S_{12} = S_{23}$, $S_{13} = S_{22}$, and $S_{14} = S_{24}$; consequently, the constellation is exactly the same as that of $\pi/4$-rotated QPSK.

TABLE I
ENVELOPE UNIFORMITY FOR NONCOHERENT DS-CDMA SCHEMES WHEN AN FIR FILTER IS USED AS A PN CHIP PULSE-SHAPING FILTER

PN Modulation	QPSK	OQPSK	NWQPSK
σ/η (%)	34.1	32.3	26.3
PMEPR (dB)	6.2	5.4	4.1
DR (dB)	48.9	43.5	11.0

V. SIMULATION RESULTS

To test the envelope uniformity of NWQPSK and CWQPSK when a spectrally efficient PN pulse shape is used, we performed simulations. In our simulations, we use a finite impulse response (FIR) filter with the impulse response of [5] as a pulse shaping filter. This FIR filter is a low-pass filter with the passband $0 \le f \cdot T_c \le 0.4801$ and the stopband $f \cdot T_c \ge 0.6022$. The maximum permissible passband ripple is ± 1.5 dB and the stopband is down -40 dB from the passband [5]. The level of envelope uniformity is measured in three ways: the standard deviation-to-mean envelope level ratio (σ/η), the peak-to-mean envelope power ratio (PMEPR), and the dynamic range (DR) of envelope power. PMEPR is defined as the ratio between the maximum and the mean envelope powers of the transmitted signal, and DR is defined as the ratio between the maximum and the minimum envelope powers of the transmitted signal. These are both important parameters for designing a power amplifier. Since the above two performance measures both involved the peak envelope value, we consider another measure independent of the this value, and defined as the ratio between the standard deviation and the mean of the envelope of the transmitted signal.

Results for QPSK, OQPSK, and NWQPSK PN modulation with noncoherent DS-CDMA systems are listed in Table I, and their constellations are shown in Fig. 6(a)–(c). From the data in Table I, one can find that the NWQPSK has better envelope uniformity than either conventional QPSK or OQPSK. In particular, the DR of NWQPSK is reduced by over 30 dB compared to that of the conventional schemes. From Fig. 6(c), it is seen that the NWQPSK has no constellation points in

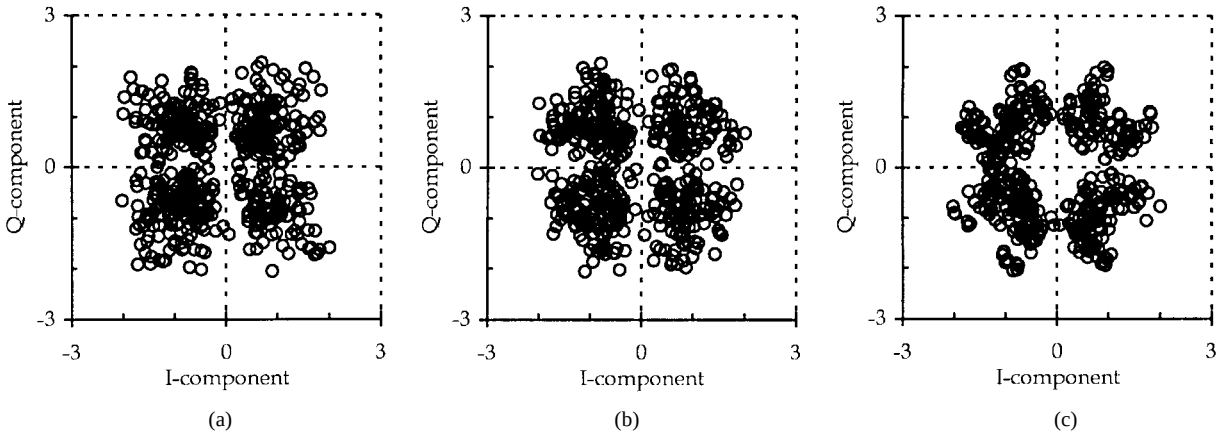

Fig. 6. Signal constellations for noncoherent DS-spread-spectrum systems with PN modulations of (a) QPSK, (b) OQPSK, and (c) NWQPSK when an FIR filter is used as a pulse-shaping filter.

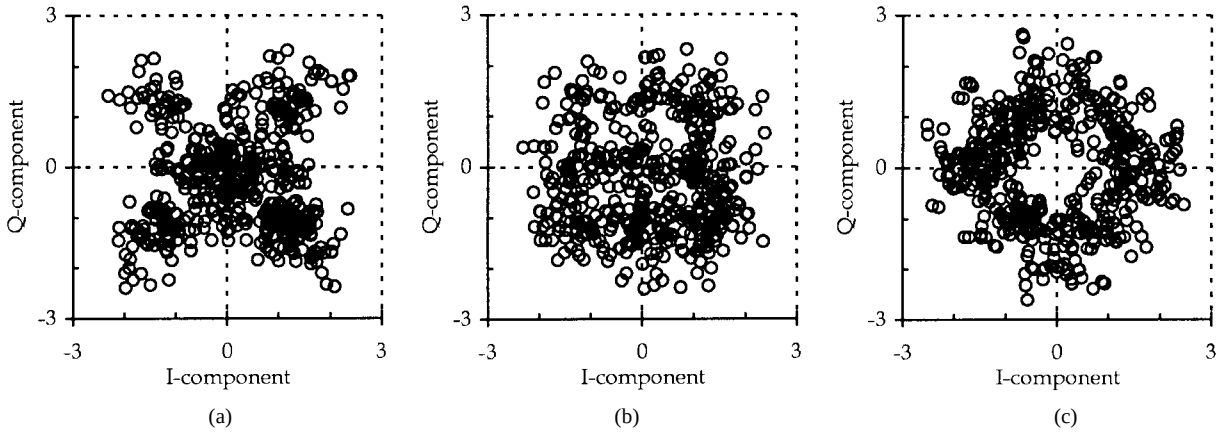

Fig. 7. Signal constellations for coherent DS-spread-spectrum systems with PN modulations of (a) QPSK, (b) OQPSK, and (c) CWQPSK when an FIR filter is used as a pulse-shaping filter and $S_D = 4S_P = 1$.

the vicinity of the origin, while Fig. 6(a) and (b) shows that is not the case for the other two schemes. Since the impulse response of the FIR filter spans $12T_c$, the amplitude of the envelope is dependent on the polarities of the last 12 PN chips. Due to the independence between the two PN sequences spreading the in-phase and quadrature data used in QPSK and OQPSK schemes, the amplitudes of the in-phase and quadrature components can have either large or small values simultaneously. However, in the NWQPSK scheme, one of the polarities of the in-phase and quadrature PN sequences always changes. This feature of NWQPSK prevents both the in-phase and quadrature components from having either large or small values simultaneously.

We also performed simulations for coherent DS-CDMA systems. Results of the QPSK, OQPSK, and CWQPSK PN modulation schemes for coherent DS-CDMA systems are listed in Table II, and their constellations are shown in Fig. 7. From the data in Table II, it can be seen that CWQPSK has better envelope uniformity than the conventional QPSK and OQPSK PN modulation schemes. Also, the DR of CWQPSK is reduced by over 40 dB relative to that of conventional schemes. For the same reason as was the case with NWQPSK, the CWQPSK has no constellation points in the vicinity of the origin [see Fig. 7(c)].

TABLE II
ENVELOPE UNIFORMITY FOR COHERENT DS-CDMA SCHEMES WHEN $S_P = S_D/4$

Pulse shaping filter	FIR			rectangular		
PN Modulation	QPSK	OQPSK	CWQPSK	QPSK	OQPSK	CWQPSK
σ / η (%)	49.5	38.0	29.4	50.0	33.9	0
PMEPR (dB)	7.9	6.5	5.4	2.6	2.6	0
DR (dB)	66.2	58.2	18.9	9.5	9.5	0

Finally, note that from Tables I and II, the envelope variation of CWQPSK is also smaller than that of noncoherent QPSK and OQPSK, even though with CWQPSK signals the pilot and the signal channels are summed, while in the noncoherent QPSK and OQPSK schemes there is no pilot channel.

VI. CONCLUSION

In this paper we proposed two Walsh-QPSK PN modulation schemes, namely NWQPSK and CWQPSK, for a noncoherent and a coherent DS-CDMA system, respectively. When a rectangular-shaped PN chip pulse is used, the NWQPSK has a similar constellation to that of the OQPSK, but there is no self-interference between the in-phase and quadrature

components since the former scheme uses two orthogonal sequences in spreading the in-phase and quadrature data. Also, the CWQPSK has a constant envelope even though the pilot channel is added to the signal channel.

When a spectrally efficient shaped PN chip pulse is used, both NWQPSK and CWQPSK have smaller envelope variations than do conventional OQPSK and QPSK PN modulation schemes. The NWQPSK and the CWQPSK PN modulation schemes, consequently, represent power-efficient structures for both noncoherent and coherent DS-CDMA systems.

REFERENCES

[1] K. S. Gilhousen *et al.*, "On the capacity of a cellular CDMA system," *IEEE Trans. Veh. Technol.*, vol. 40, pp. 303–312, May 1991.

[2] A. Fukasawa *et al.*, "Wideband CDMA system for personal radio communications," *IEEE Commun. Mag.*, vol. 34, pp. 116–123, Oct. 1996.

[3] A. Baier *et al.*, "Design study for a CDMA-based third-generation mobile radio system," *IEEE J. Select. Areas Commun.*, vol. 12, pp. 733–743, May 1994.

[4] V. K. Grag and E. L. Sneed, "Digital wireless local loop system," *IEEE Commun. Mag.*, vol. 34, pp. 112–115, Oct. 1996.

[5] EIA/TIA/IS-95, "Mobile station-base station compatibility standard for dual-mode wideband spread spectrum cellular system," July 1993.

[6] J. Boccuzzi, "Performance evaluation of nonlinear transmit power amplifiers for North American digital cellular portables," *IEEE Trans. Veh. Technol.*, vol. 44, pp. 220–228, May 1995.

[7] K. I. Kim, "On the error probability of a DS/SSMA system with a noncoherent M-ary orthogonal modulation," in *Proc. Vehicular Technology Conf.*, Denver, CO, 1992, pp. 482–485.

[8] J. L. Shanks, "Computation of the Fast Walsh-Fourier Transform," *IEEE Trans. Computers*, vol. C-18, pp. 457–459, May 1969.

[9] M. K. Simon *et al.*, *Spread Spectrum Communications.* Computer Science Press, 1985.

Dongwook Lee (S'87–M'92) received the B.E., M.E., and Ph.D. degrees from Yonsei University, Seoul, Korea, in 1984, 1986, and 1991, respectively.

From 1991 to 1992 he was a Lecturer with the Department of Electrical Engineering, Yonsei University, Seoul, Korea. Since June 1992 he has been with Electronics and Telecommunications Research Institute (ETRI), Taejon, Korea, where he is a Senior Engineer, working in the area of mobile communications. From 1996 to 1998 he was also a Visiting Assistant Project Researcher with the University of California at San Diego, La Jolla, CA.

Dr. Lee was the recipient of a scholarship from Johan Cho Foundation, Korea, in 1983. In 1992 he received the 2nd Prize of Chunkang Award from the Chunkang Foundation, Korea.

Hun Lee received the B.S. degree from Seogang University, Seoul, Korea, in 1978, and the M.S. degree from the Korea Advanced Institute Science and Technology (KAIST), Seoul, Korea, in 1981.

In 1981 he joined the Electronics and Telecommunications Research Institute (ETRI), Taejon, Korea, where he is currently a director of Mobile Communications Technology Department. His current research interests and projects are mainly concentrated on the digital cellular and personal communication technologies.

Laurence B. Milstein (S'66–M'68–SM'75–F'85), for photograph and biography, see p. 654 of the May 1998 issue of this TRANSACTIONS.